Boundary Extraction and Polarimetry in Translucent Specimens for Photoelastic Stress Analysis

Ahmed Ghali[1], Tony P. Pridmore[1], I. Arthur Jones[2], Peiji Wang[2] and Adib A. Becker[2]
[1]School of Computer Science and IT, University of Nottingham, Nottingham, NG1 8BB, UK
[2]School of Mechanical, Materials, Manufacturing Engineering and Management, University of Nottingham, Nottingham, NG1 8BB, UK

ABSTRACT

We address the problem of providing input to a novel method of interpreting photoelastic data for performing experimental stress analysis of models of engineering components. This method employs conventional photoelastic data relating to the directions of the principal stresses in the specimen (isoclinic data), along with the difference in principal stresses (isochromatic data). Both are used within an inverse boundary element model to reconstruct the load conditions at the model boundary and hence to recover the principal stresses in the specimen without recourse to numerical integration of shear stress gradient. We describe methods of obtaining unwrapped isoclinic and isochromatic phase maps from sequences of images captured within a computer-controlled polariscope. A boundary element model of the specimen, congruent with the isoclinic and isochromatic phase maps, is obtained from an image captured within the polariscope under either traditional lighting conditions or by configuring the polariscope to provide a light field background. Image segmentation reveals the boundary of the specimen, which is then described in terms of simple geometric primitives. Boundary points and geometric descriptions are both used to produce the final boundary element model. The techniques described have been applied to a number of contact specimens; results are presented and discussed.

Keywords: stress analysis, photoelasticity, image segmentation, boundary representations

1. INTRODUCTION

Photoelasticity is a long-established technique for experimental stress analysis in mechanical engineering and related disciplines. While the physical phenomenon of photoelasticity was observed in the mid 19th century, its use for engineering stress analysis dates from the 1930s for the analysis of two-dimensional engineering specimens, and subsequent extensions (notably the frozen stress method, which uses 2D slices cut from a 3D model) made it a valuable approach to the analysis of 3D specimens. The technique is of particular value in the analysis of specific situations such as contact and for the validation of numerical models.

The principle of photoelasticity is as follows. When a ray of light enters a specimen made from a suitable photoelastic material e.g. epoxy resin or polycarbonate, it is split into two mutually perpendicular polarised components that are aligned with the axes of the principal stresses σ_1 and σ_2 of the component. These wave components propagate through the specimen at different velocities depending upon the difference in principal stress within the specimen. On emerging from the specimen, these wave components recombine to form a light ray with different polarisation properties from the ray initially entering the specimen. By placing the specimen within a polariscope (Figure 1) consisting of a number of adjustable elements with different optical properties, measurements of light intensity and/or its variation may be obtained from which the relative retardation of the specimen and the orientation of the principal axis system can be estimated. This normally involves the identification of loci of constant principal stress direction (isoclinic data) and constant relative retardation (isochromatic data). Photoelasticity generates images comprising two interwoven patterns of fringes, with the isoclinics being visible as relatively dark regions and the isochromatics appearing as regions of constant colour. Photoelastic stress analysis does not directly yield the individual values of principal stress; only the difference, $\sigma_1-\sigma_2$, in principal stresses is obtained. Some rather tedious numerical integrations must be performed if σ_1 and σ_2 are to be recovered from the relative retardation (which is proportional to $\sigma_1-\sigma_2$). This process is known as stress separation.

Computational Imaging, Charles A. Bouman, Robert L. Stevenson, Editors,
Proceedings of SPIE-IS&T Electronic Imaging, SPIE Vol. 5016 (2003)

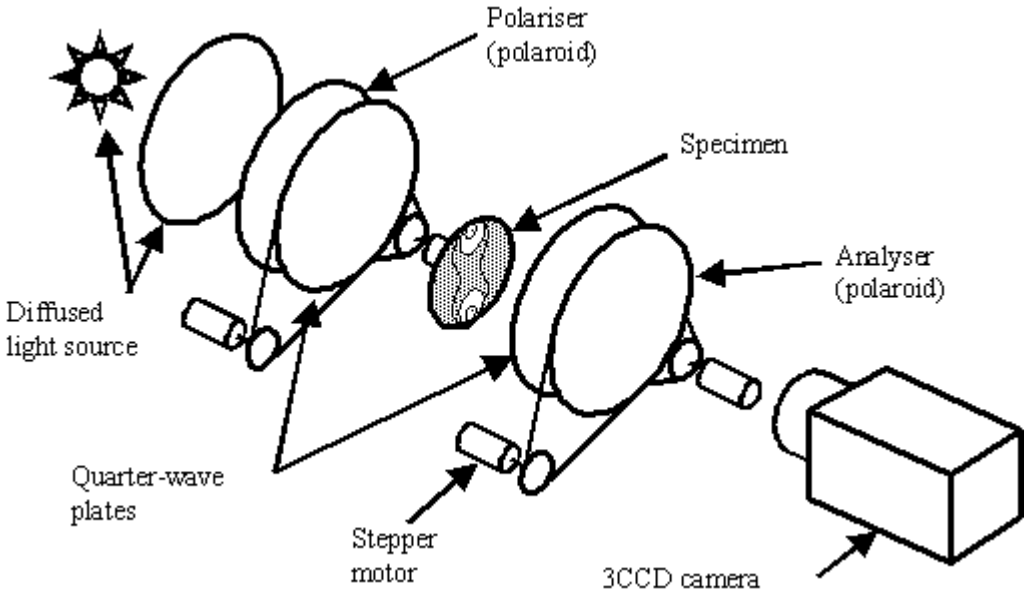

Figure 1. A digital imaging polariscope.

Manual photoelasticity is a laborious exercise, and a great deal has been published on the automation of the process. Four main approaches have been adopted:

• Automation of manual methods of photoelasticity on a point-by-point basis e.g. Fessler *et al* [1]. This is an acceptable approach for collecting data relating to small numbers of points, but impractical where measurements are needed at many points.

• Methods based upon recognition of the unique colour associated with each value of isochromatic fringe e.g.. Ajovalasit *et al* [2]. There are however issues regarding the robustness and generality of this approach since the colour of photoelastic specimens can vary.

• Methods based upon the thinning and/or multiplication of fringe patterns in order to identify their centres e.g. Seguchi *et al* [3]. While this draws upon established techniques in image processing, it is of limited use where it is desirable to recover non-integer fringe values at specific points.

• Methods based upon sequences of images captured under different polariscope settings, e.g. the phase-stepping approaches of Hecker and Morsche [4] and of Patterson and his co-workers e.g. [5]. It is desirable here to aim for the highest possible accuracy and to minimise any tendency towards ill-conditioning of the analysis calculations. The approach followed here is therefore to use a least-squares approach to the solution of an overdetermined set of equations, and to capture the isoclinic data separately from the data to be used for determining the isochromatic data.

A novel approach to stress separation has been developed [6] which involves the use of conventional photoelastic data relating to the directions of the principal stresses σ_1 and σ_2 in the specimen (isoclinic data), along with the value of the difference $(\sigma_1-\sigma_2)$ in principal stresses (isochromatic data). The main novelty of the task involves using these data within an inverse boundary element model to reconstruct the load conditions at the boundary of the model and hence perform "stress separation" in order to recover the individual values of σ_1 and σ_2 in the specimen without recourse to

the usual (error-sensitive) numerical integration of shear stress gradient. The method requires a variety of information to be extracted from digital images captured with in polariscope, specifically:

- Unwrapped phase maps giving the direction of the principal stresses in the specimen (isoclinic data).
- Unwrapped phase maps giving the birefringence (relative retardation) of the specimen expressed as whole and fractional fringe values (isochromatic data)
- Data describing the geometry of the edge of the specimen so that a boundary element model of the specimen may be constructed which is congruent with the isoclinic and isochromatic phase maps.

Section 2 presents methods of obtaining unwrapped isoclinic and isochromatic phase maps from sequences of images captured within a computer-controlled polariscope, while section 3 focuses on the formation of the required boundary model. The result of a case applying the finished system to a realistic engineering case study are then given in Section 4 before conclusions are drawn in section 6.

2. PHOTOELASTIC ANALYSIS AND PHASE UNWRAPPING

The isoclinic and isochromatic phase maps are both obtained from sequences of images captured using a computer-controlled polariscope with video camera and framegrabber. In order to keep experimental error to a minimum, a new phase-stepping strategy has been adopted which captures overdetermined data sets and performs a least-squares fit to an optical model of the apparatus and specimen.

The isoclinic data giving directions of the principal stresses in the specimen are obtained by analysing the phase of variations in light over a sequence of images captured using a polarisation-stepped crossed plane polariscope. In other words, a pair of crossed polarising elements are stepped through 90° and the phase angle of the light variation over this sequence is used to calculate the isoclinic angle in the range 0-90°. The goodness-of-fit of the intensity data to the assumed sinusoidal variation is also quantified via a map of the coefficient of determination (R^2) for use as described below. The light variations repeat identically for every 90° of polariscope rotation, so the isoclinic angle can only be determined directly within an undefined quadrant. In order to resolve this ambiguity, phase unwrapping is required.

In order to capture the isochromatic data, a new phase-stepping strategy has been adopted which configures the polariscope as a generator of a wide variety of polarisation states (represented as the vertices of a polyhedron on the Poincare sphere) following approaches borrowed from other branches of polarimetry. An overdetermined least-squares approach is then used, in conjunction with the unwrapped isoclinic map, to reconstruct the map of relative retardation (isochromatic data) of the photoelastic specimen. Once again, this map of data is expressed in "wrapped" form (fractional part only, i.e. fringe values in the range 0-1) requiring the integer part of the fringe orders to be recovered by unwrapping.

Phase unwrapping refers to the conversion of a phase map from its "wrapped" or modulo form with sharp discontinuities into "unwrapped" form where the values are continuous. For example, a continuously-varying phase angle may initially be measured in the range 0-2π radians, with the readings "jumping" from 2π back to zero each time the phase angle increases beyond a multiple of the wrapped range. Unwrapping of such a phase map involves reconstructing the multiple of 2π which must be added or subtracted at each point to obtain the continuously-varying quantity. An excellent overview of unwrapping is presented by Ghiglia and Pritt [7], and several of the algorithms they present have been evaluated for use within the present problem. Here, both the isoclinic (principal stress direction) and isochromatic (principal stress orientation) data require unwrapping since the approaches described early result in isoclinic maps presented in the range 0°-90° and isochromatic maps with relative retardations in the range 0-1 fringe orders (wavelengths of relative retardation).

A variety of published approaches may be used for unwrapping the isoclinic data, but particular promise has been shown by the use of a quality-guided algorithm published by Ghiglia and Pritt which makes use of the coefficient of determination (R^2) characterising the goodness of fit of the isoclinic data to the available images, enabling regions of poor quality to be avoided in the unwrapping process. Strictly speaking, the "unwrapped" isoclinic maps are should be

re-wrapped into a range of 0-180°, although spurious multiples of 180°are ignored in all subsequent calculations on the isoclinic angle.

The quality-guided algorithm has also been evaluated for the unwrapping of the isochromatic data, although it has shown no great advantage over (for example) Goldstein's branch-cut method as presented by Ghiglia and Pritt.

With knowledge of the calibration constant of the photoelastic material and the specimen thickness, the isochromatic phase map is converted into units of stress. In combination with the principal stress direction information contained in the unwrapped isoclinic map, and using the tensor transformation for in-plane stresses (known to engineers as the Mohr's circle transformation for stresses), the Cartesian stress difference $\sigma_x - \sigma_y$ and the shear stress τ_{xy} are calculated for every pixel position to be used within the inverse boundary element model. It is however first necessary to define the boundary element model geometry.

3. OBTAINING A BOUNDARY MODEL

With the polarizer and analyzer engaged for photoelastic analysis, the polariscope produces complex colour images in which the low contrast specimen boundary is extremely difficult to locate to the accuracy required. Images captured within the polariscope but under traditional lighting conditions (i.e. without passing the illuminant through the polarising optical elements) or by configuring the polariscope to provide a "light field" background will, however, give reasonable contrast.

Figure 2 shows a selection of images captured against a light field background. To achieve the spatial resolution required for the photoelastic analysis, viewing distance varies considerably. In some cases, e.g. figure 2a, the specimen will dominate the image. In others, e.g. figure 2d, the specimen occupies a relatively small proportion of the image, with many extraneous components of the polariscope also visible. Variations in material also affect the image, while the specimens in figure 2a and b are distinguished by clearly visible colour patterns, those in figures 2c and d are much more uniform in appearance.

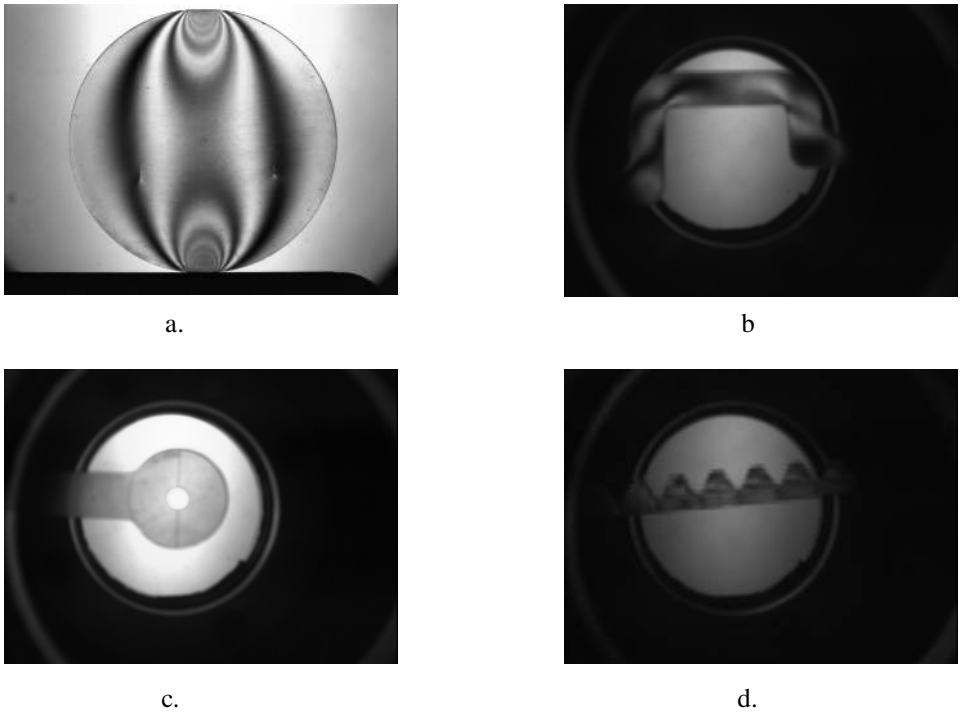

a. b

c. d

Figure 2. A selection of polariscope images captured against a light field background.

In the proposed technique a background image showing only the light field illuminated polariscope is first subtracted from an image captured with a specimen in place. The resulting difference image is then thresholded to identify the specimen. Figure 3 shows the background image used in the examples presented here.

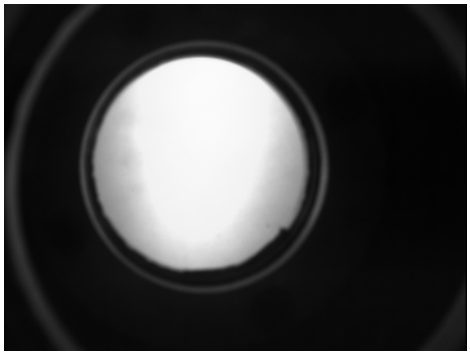

Figure 3. Background image of a light field illuminated polariscope.

The goal of this project is to support, rather than replace, the engineer in his/her analysis of a given specimen. While it is anticipated that a higher degree of automation may be introduced in the future, in the current implementation the operator selects all threshold values via a graphical user interface. The user is also free to choose between converting the input colour images to grey level before subtraction or to subtract and threshold differences between colour data. In the experiments performed to date the latter route has demonstrated a greater resilience to image noise. Figure 4 shows the result of applying this procedure to the images of figure 2.

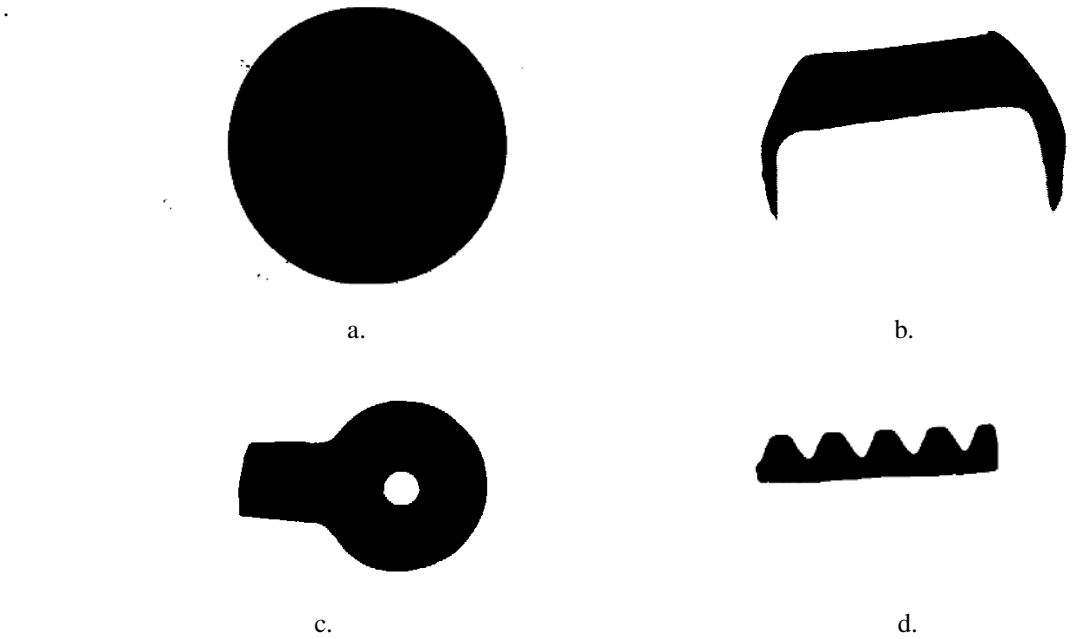

Figure 4. The result of segmenting the images of figure 2 to identify the specimen.

After segmentation a binary image is produced in which specimen points are black and background pixels white (figure 4). Noise is then reduced by a series of logical filters that identify and remove small white holes and extraneous black "objects".

Black/white boundaries are extracted and interactively smoothed. Smoothing is achieved via repeated application of mean or Gaussian weighted filtering. The user must decide how much filtering to apply to achieve an acceptable balance between smooth boundary segments and clear discontinuities. Local curvature estimates are then computed and used to support the identification of lines and arcs. An automatic threshold provides a first estimate, which the user can interactively modify if he/she chooses. During this process the boundary representation is overlaid on the original data to allow the user to judge the quality of the results obtained and respond accordingly. Finally, each straight line and curve segment is subdivided to produce a boundary element model.

Boundary points and geometric descriptions are both used to produce the boundary element model. The number and size of elements required are determined automatically for each line. The number of elements within each line may, however, be modified interactively to meet the requirements of the subsequent analysis. Element sizes are then modified so that the size of the end element on one line segment equals the size of the start element on the next. A grading factor is calculated for each line so that the elements on a line increase or decrease smoothly either in length (for a straight line element) or in angle (for a curved element). Figure 5b shows the boundary element model extracted from the image of Figure 5a. The boundary element model is finally used within an inverse analysis to recover the contact conditions (contact pressure and frictional stress distributions) between the gear tooth shown and the tooth with which it meshes.

a.

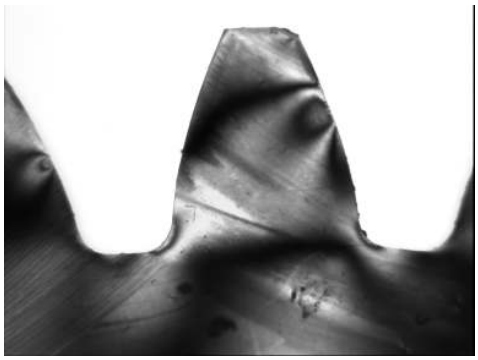

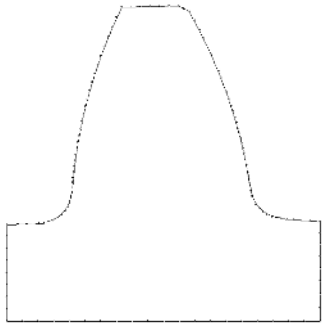

b.

Figure 5. The final boundary element model (b) extracted from a colour polariscope image (a). Note that this image has been manually trimmed to isolate the region of engineering interest.

4. RESULTS

The test geometry chosen was a 38-tooth, 4.2 module spur gear with 25mm face width also being studied under a separate programme sponsored by British Gear Association and Rolls-Royce plc. A pair of frozen-stress models were finish ground from near net shape blanks cast from CIBA CT-1200-1 epoxy resin using CIBA 907 hardener, and were loaded in a rig designed to compensate the centre distance of the meshing pair to take account of the very large expansion of epoxy resin during the stress-freezing cycle. The results of the analysis are summarised in Figures 6 and 7. These show that the separated internal stresses and contact conditions in a photoelastic model of an engineering component can be recovered by the techniques developed within the present project. Comparison of Figures 6(e) and 6(i) show that the map of $\sigma_1 - \sigma_2$ generated by a forward BE analysis using the reconstructed boundary conditions agrees with the unwrapped isochromatic map very closely – in other words, the photoelastic data have been correctly interpreted. Figure 7 shows that the normal stresses obtained from the reconstructed boundary values agree closely with a simple calculation of Hertz contact stress, with the reconstructed values lying (as expected) between the upper and lower bounds arising from assuming that the load is carried respectively by one contacting tooth pair alone and by sharing between two tooth pairs.

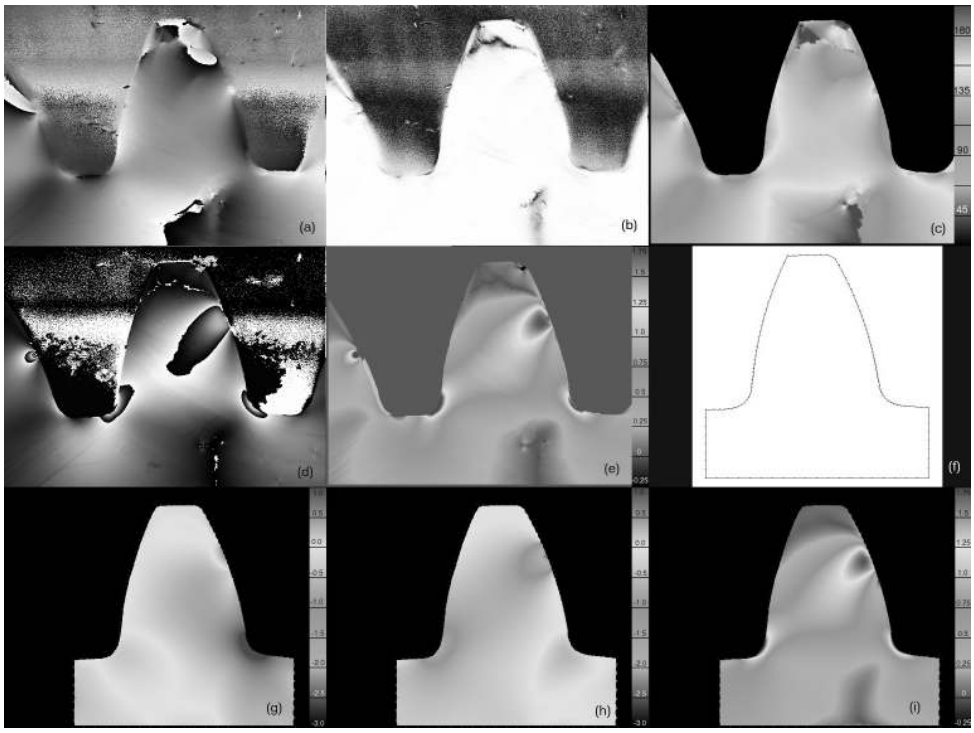

Figure 6: images obtained from frozen-stress analysis of gear. (a) Isoclinic map obtained prior to unwrapping (black=0º, white=90º). (b) Quality (R^2) map relating to isoclinic data (black=0, white=1). (c) Isoclinic map unwrapped using quality approach, shown in false colour, background blanked. (d) Wrapped isochromatic map (from green colour plane: fringe order goes from 0 to 1 as greyscale goes from black to white). (e) Unwrapped isochromatic map shown in false colour: background blanked for comparison with (i). (f) Boundary element model fitted to a portion of the gear model. (g) σ_1 data recovered from inverse BE method expressed as a false colour map (in units of fringe order). (h) σ_2 data recovered from inverse BE method expressed as a false colour map (in units of fringe order). (i) $\sigma_1-\sigma_2$ data recovered from inverse BE method expressed as a false colour map (in units of fringe order) for comparison with Figure 2(e) Note that the BE formulation does not permit "internal" stress points to be placed right up to the model boundary, so that reconstructed maps (g) to (i) do not reach quite to the edge of the specimen.

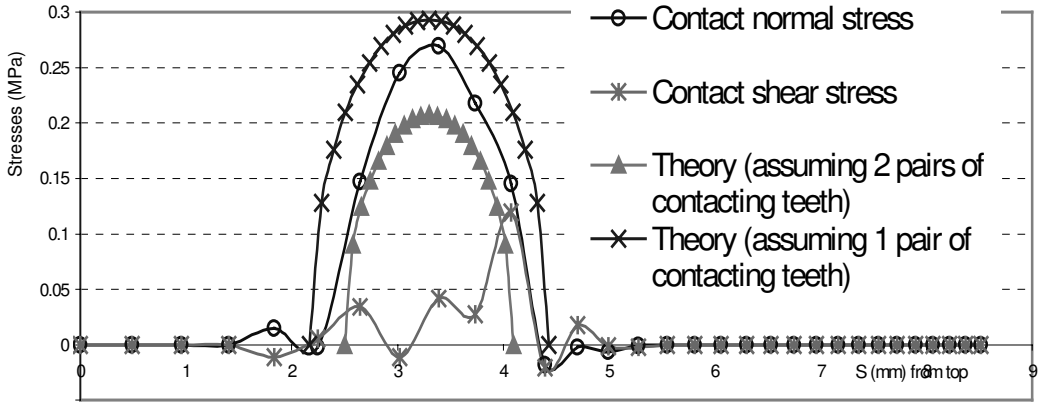

Figure 7: Profile of contact stresses recovered for contact region of gear teeth, showing comparison between recovered contact normal stress and that obtained from Hertz contact theory for the given loads and experimentally-measured specimen properties.

5. CONCLUSION

A novel approach to the stress separation of photoelastic results has been developed which includes the recovery of contact stresses using a variation upon boundary element analysis combined with a range of digital imaging techniques. The successful implementation of a novel inverse BE method is expected to lead to further expansion of this computational technique into other types of inverses stress analysis in which internal stress or strain data are measured by methods other than photoelasticity. Industries, such as aerospace and automotive, who rely on accurate data from experimental stress analysis techniques will benefit from this research. Furthermore, manufacturers of experimental stress/strain measurement devices will benefit from the interaction of inverse techniques and automatic data acquisition software. The current boundary extraction system is highly interactive, further automation is currently being explored, incorporating an improved automatic background image subtraction technique and a recursive contour segmentation/description technique.

ACKNOWLEDGEMENTS

This research was supported by EPSRC Standard Research Grant GR/M40684/01, "Digital Photoelasticity of Complex Geometries and Loads using Boundary Integral Stress Separation".

REFERENCES

1. H. Fessler, R. E. Marston and E. Ollerton, "A micropolariscope for automatic stress analysis", *J. Strain Analysis*, 22, 22-35.

2. A. Ajovalasit, S. Barone and G. Petrucci, "Towards RGB photoelasticity: full-field automatic photoelasticity in white light", *Experimental Mechanics*, 35(3), 193-200. 1995.

3. Y. Seguchi, Y. Tomita and M. Watanabe, "Computer-aided fringe pattern analyzer – a case of photoelastic fringe". *Experimental Mechanics*, 362-370, 1979

4. F.W. Hecker and B. Morsche, "Computer measurement of relative retardations in plane photoelasticity". In Weiringa, H (ed.), *Experimental Stress Analysis*, Nijhoff, The Netherlands, pp. 532-542, 1986.

5. E. A. Patterson and Z. F. Wang, "Towards full field automated photoelastic analysis of complex components", *Strain*, 49-53, 1991.

6. D. Chen, A.A. Becker, I.A. Jones, T.H. Hyde and P. Wang, "Development of new inverse boundary element techniques in photoelasticity", *Journal of Strain Analysis*, 36, 3, pp 253-264, 2001.

7. D.C. Ghiglia, and M.D. Pritt, *Two-dimensional phase unwrapping: theory, algorithms and software* Wiley, New York, 1998.